Behavior of a Moored LNG Ship in Swell Waves

W. van der Molen[1]; H. Ligteringen[2]; J. C. van der Lem[3]; and J. C. M. de Waal[4]

Abstract: In the design of oil and gas terminals, six degrees of freedom (SDF) models are often used to calculate the motions of the moored ship and forces in mooring lines and fenders. Although the SDF simulation programs have been used for more than 20 years, there is still little verification of the results with prototype measurements. This paper includes the results of a verification of one of these SDF models using prototype measurements as reference data. The prototype measurements consisted of mooring line loads of liquefied natural gas (LNG) carriers at berth for periods during which environmental conditions were recorded. A study was carried out to simulate these conditions in the model and to compare the model results with the measurements. In addition to mooring line loads, the computed vessel motions have been analyzed. For the studied berth situation, the yaw motion resulting from swell waves is quite dominant and is causing large breast line forces. An empirical expression has been derived to calculate the yaw motions of the moored LNG carrier in swell waves. This expression is a first step in defining a general expression to estimate maximum yaw motions and mooring forces to be used in preliminary harbor design.

DOI: 10.1061/(ASCE)0733-950X(2003)129:1(15)

CE Database keywords: Ships; Waves; Mooring.

Introduction

Research in the 1970s and early 1980s on the behavior of moored ships in waves has led to the development of several computer models that calculate wave forces, motions of the moored ship, and forces in fenders and mooring lines. The models are so-called six degrees of freedom (SDF) models because forces and motions of the ship are calculated in the six degrees of freedom. In this period several models have been set up and further developed. One of those models is TERMSIM, developed by the Maritime Research Institute Netherlands (MARIN) in Wageningen. This model is used widely in the industry as a design tool for oil and gas jetties, SBMs, and MBMs. In the design process the TERMSIM simulation program is used to calculate vessel motions and forces in mooring lines and fenders based on ship and jetty characteristics and environmental conditions. For proper modeling the layout of the mooring facility, as well as spring constants of mooring lines and fenders, needs to be defined. The simulation runs carried out in the design process on several design ships provide directions to improve and optimize the layout of the mooring facility, including positions of loading arms and mooring and breasting dolphins.

In the past extensive validation of SDF models has been done by comparing the calculated results to scale model measurements, for example, as described by van Oortmerssen et al. (1986). This verification was done as a validation study of the program MOORSIM, a predecessor of the TERMSIM program. Simulation models are in this way validated to minimize the differences with measurements. Besides the comparison to scale model tests, not much is done on validation with use of prototype measurements. Further verification of the TERMSIM model with the prototype situation under the existing conditions would increase the reliability of the model.

Although the SDF models have been shown to be a useful tool in the detailed design of mooring facilities, they are generally too complex to be of use in the initial stage of a terminal design, that is, the conceptual or preliminary design stage. For this reason the research project, ‘‘Behavior of Moored Ships in Long Waves,’’ has been initiated by Delft University of Technology. The objective of this research program is to develop simplified expressions to calculate vessel motions and maximum loads in mooring lines and fenders for the evaluation of port layouts in the preliminary design stage. Earlier research on such simplified expressions is presented in two papers (Mol et al. 1986; Ligteringen and Moes 2001). The advantage of such simplified expressions over the use of SDF models is that these are easy and quickly applicable and therefore can be appropriate in the preliminary design stage, taking into account the large variation and uncertainties in the design parameters.

This paper gives a few mathematical principles of the SDF model TERMSIM and describes the verification study of the program TERMSIM with measured data (van der Molen 2001). The model was verified using prototype measurements consisting of mooring line forces that were monitored at Woodside’s liquefied natural gas (LNG) loading terminal in Withnell Bay, West Australia. Based on the study results, it was concluded that yaw mo-

[1]Delft University of Technology, Faculty of Civil Engineering and Geosciences, Stevinweg 1, P. O. Box 5048, 2600 GA Delft, The Netherlands.

[2]Head Section on Harbours and Waterways, Delft Univ. of Technology, Faculty of Civil Engineering and Geosciences, Stevinweg 1, Box 5048, 2600 GA Delft, The Netherlands.

[3]Royal Haskoning, Heer Bokelweg 145, P. O. Box 705, 3000 AS Rotterdam, The Netherlands.

[4]Sakhalin Energy Investment Company Ltd., Visseringlaan 25, P. O. Box 60, 2280 AB Rijswijk, The Netherlands.

Note. Discussion open until June 1, 2003. Separate discussions must be submitted for individual papers. To extend the closing date by one month, a written request must be filed with the ASCE Managing Editor. The manuscript for this paper was submitted for review and possible publication on January 15, 2002; approved on July 10, 2002. This paper is part of the ***Journal of Waterway, Port, Coastal, and Ocean Engineering***, Vol. 129, No. 1, January 1, 2003. ©ASCE, ISSN 0733-950X/2003/1-15–21/$18.00.

tions were governing for the given berth orientation, and an expression to calculate yaw motions of the moored ship is described. Conclusions have been drawn about the resemblance of simulations to prototype measurements and the usefulness of the derived formula.

Mathematical Model

Equations of Motion

The motions of moored objects under the influence of arbitrary external forces can be determined from the solution of the following equations of motion (van Oortmerssen 1976):

$$\sum_{j=1}^{6}\left\{(M_{kj}+m_{kj})\cdot\ddot{X}_j(t)+\int_{-\infty}^{t}R_{kj}(t-\tau)\cdot\dot{X}_j(\tau)\cdot d\tau\right.$$
$$\left.+C_{kj}\cdot X_j(t)\right\}=F_k(t);\quad k=1,2,...6 \tag{1}$$

where X_j=motion in j mode; t,τ=time; M=inertia matrix; m=added inertia matrix; R=matrix of retardation functions; C=matrix of hydrostatic restoring forces; and F_k=time-varying external force in k mode.

The left-hand side of Eq. (1) contains the rigid body motions and linear hydrodynamic reaction forces only. The latter forces are generated by the motions of the floating body and are described by the retardation functions. The external forces generally contain contributions that are nonlinear functions and also are a function of the vessel motions, thus requiring the equations of motion to be solved in the time domain using numerical techniques. The nonlinear terms are mainly due to the nonlinear characteristics of fenders and mooring lines, second-order wave forces, and nonlinear drag.

Loads on Moored Ship

The external forces on the moored ship consist of the following terms: (1) wave forces; (2) current forces; (3) wind forces; (4) mooring line forces; and (5) fender forces.

The mooring line forces and fender forces are calculated based on the characteristics of the mooring lines and fenders. The wave forces are divided into first-order and second-order forces. The first-order forces are calculated from summation over all wave frequencies using first-order transfer functions:

$$F^{(1)}(t)=\sum_{i=1}^{N}\hat{\zeta}_i\cdot\hat{F}_{\zeta}^{(1)}(\omega_i)\cdot\cos[\omega_i t+\varphi^{(1)}(\omega_i)+\epsilon_i] \tag{2}$$

where $F^{(1)}(t)$=first-order wave force; $\hat{\zeta}_i$=wave amplitude; ω_i=wave angular frequency; ϵ_i=random phase angle (between 0 and 2π rad); $\hat{F}_{\zeta}^{(1)}(\omega_i)$=amplitude of first-order transfer function; and $\varphi^{(1)}(\omega_i)$=phase angle of first-order transfer function.

The low frequency second-order wave drift forces, which are linked to wave grouping, are expressed using second-order transfer functions based on two frequencies. These quadratic functions are used to calculate the spectral density of the wave drift forces in the frequency domain based on the pressure integration formulation (Pinkster 1980). Then the second-order wave force as a function of all combinations of the two frequencies is constructed using direct summation techniques as follows:

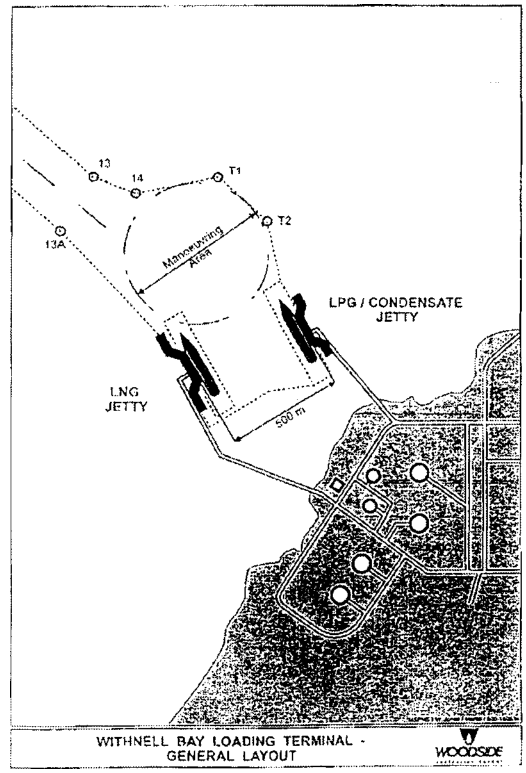

Fig. 1. Layout of Withnell Bay gas loading terminal

$$F^{(2)}(t)=\sum_{i=1}^{N}\sum_{j=1}^{M}\hat{\zeta}_i\hat{\zeta}_j\{P_{ij}\cos[(\omega_i-\omega_j)t+(\epsilon_i-\epsilon_j)]$$
$$+Q_{ij}\sin[(\omega_i-\omega_j)t+(\epsilon_i-\epsilon_j)]\} \tag{3}$$

where P_{ij}=in-phase part of second-order transfer function $P(\omega_i,\omega_j)$; and Q_{ij}=out-of-phase part of second-order transfer function $Q(\omega_i,\omega_j)$.

The first- and second-order transfer functions are obtained from a hydrodynamic file, which contains matrices of hydrodynamic coefficients and first- and second-order transfer functions and is characteristics of a certain ship and water depth.

Forces in mooring lines are obtained using a quasistatic line model. Forces are calculated from the ship motions and line characteristics. Further research is required to verify the necessity of implementation of a more complete line model including line dynamics.

Simulation Tests

To verify the simulation model TERMSIM, computer simulation results are compared to prototype measurements consisting of mooring line force data and carried out on a 125,000 m^3 LNG carrier moored to a jetty. Measurements were carried out at the LNG jetty at the Withnell Bay loading terminal, located in the Mermaid Sound near the Northwest Shelf in Australia. The general layout of the terminal is presented in Fig. 1, showing the position of the LNG jetty, the dimensions of the vessels are given in Table 1, and the berth layout is given in Fig. 2. The wave direction given in Fig. 2 corresponds to the direction of the approach channel shown in Fig. 1, which appeared to be the dominant direction. The ships are equipped with 16 steel wire mooring

Table 1. Characteristics of Northwest LNG carriers

Characteristic	Symbol	Unit	Value
Displacement laden	Δ	tons	93,240.00
Displacement ballast	Δ	tons	76,636.00
Length over all	L_{OA}	m	272.00
Length between perpendiculars	L_{PP}	m	259.00
Beam	B	m	47.20
Depth	H	m	26.50
Draft laden	T	m	10.95
Draft ballast	T	m	9.00

lines with 11 m polyester tails; two Yokohama air block fenders are attached to each breasting dolphin.

Prototype Measurements

The prototype measurements consisted of line force data in each mooring line. In order to reduce the data to be saved, only three values were stored per 10 min: the average, minimum, and maximum mooring line force in each line.

In the verification analysis the dynamic behavior was studied by calculating the time-varying difference between the maximum and average force and between the minimum and average force per 10 min interval. These two parameters were used as reference data for the simulation tests thus ignoring possible small differences in the average values of measurement and simulation caused by pretension and tidal fluctuations. From the simulations the same parameters were calculated in order to be compared to the measured data.

Environmental Conditions

Environmental conditions were measured simultaneously with the line force measurements. Wind speeds were monitored using an RM Young anemometer. The measured wind was shown to be in a predominantly west from offshore direction, with a 10 min average velocity ranging from 0 to 12 m/s and a 3 s gust.

Tidal data were obtained from the Coastal Data Center, West Australia, for a location in King Bay close to the site. The tidal range is about 1.0 m during neap tide and about 3.60 m during

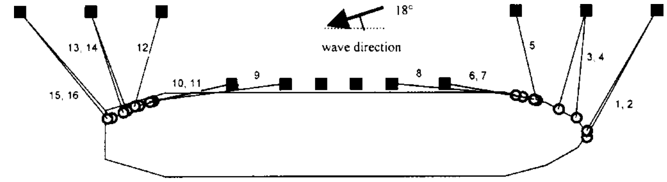

Fig. 2. Berth layout

spring tide. Current monitoring had not been done, but currents were assessed to be of the order of 0.30 m/s during neap tide and 0.65 m/s during spring tide.

Waves were monitored by a Datawell Directional Waverider just outside the harbor basin. Wave conditions are generally low (0.2 to 0.7 m H_s) and only during a storm will occasionally exceed 1.0 m. Swell waves during the measuring period range from 0.1 to 0.4 m, with peak period from 13 to 18 s. Wave conditions were well below design conditions during the entire measuring period.

From the available environmental data, a number of periods have been selected for the simulations, which can be divided into the following categories:

1. Periods with dominant (vertical tide);
2. Periods with significant wind loads combined with low-wave conditions;
3. Periods with relatively high waves (sea state, $T_p = 6$ to 7 s); and
4. Periods with relatively high waves (swell, $T_p = 14$ to 18 s).

For all these periods, environmental conditions were selected and mooring simulations executed and compared (van der Molen 2001). From these simulations it was concluded that swell waves are dominant for mooring loads at the terminal location. A typical wave spectrum that was present several times during the measured period is given in Fig. 3. Significant wave height of this spectrum is 0.27 m, and peak period is 16 s.

Results

Forty-five simulation runs have been carried out in the verification study. Nine sets of prototype measurement data were used for verification, on which a sensitivity analysis has been carried out

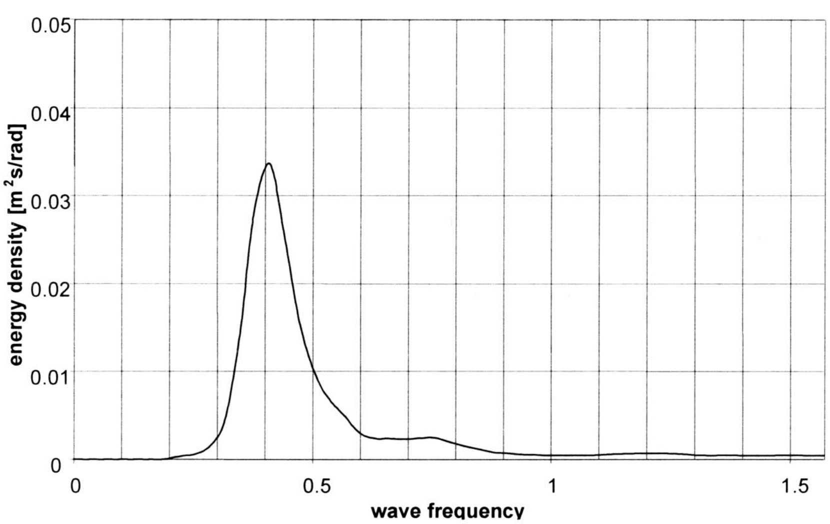

Fig. 3. Typical wave spectrum

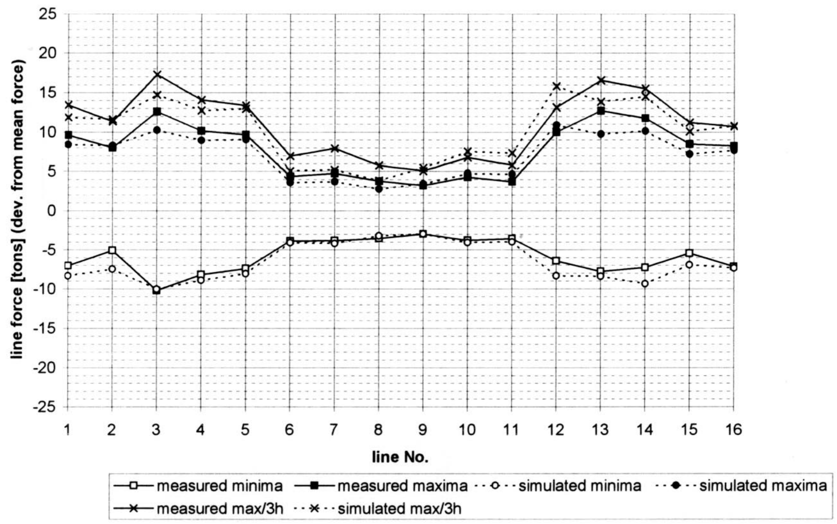

Date	Vessel	Environmental conditions		
		wind	tide	waves
2 August 1996	Standard loaded 125,000 m^3 LNG carrier 20 m water depth, T = 11.3 m	v = 7.4 m/s $\theta_v = 80°$	level = AHD +1.8 m u = 0.2 m/s $\theta_u = 120°$	$H_s = 0.28$ m $T_m = 14$ s $\theta_w = 198°$

Fig. 4. Comparison of line forces, loading condition 100%

in order to estimate the effects of the loading condition, wave direction, directional spreading of waves, and mooring line characteristics. The actual mooring arrangement and design vessel were used and input conditions selected as close as possible to prototype conditions. The calculated time series of mooring line forces was processed to allow a direct comparison of computational results with the measured data.

The following definitions have been applied in the processing and presentation of the results:

1. Minimum and maximum mooring line forces are amplitudes of (measured and calculated) forces, with the zero force defined as the mean force due to pretension and static loads such as wind, current, and mean wave drift force.
2. Because of the stochastic nature of the exciting wave forces, the 10 min minimum and maximum mooring line forces are not constant in time, but will change every 10 min. Hence, mean values of the 10 min minima and maxima of the line forces were determined based on a certain period of observations, during which environmental conditions and pretension are constant in time. These values were compared with 10 min minima and maxima of 3 h TERMSIM simulations (3 h because this is the maximum simulation period in TERMSIM).
3. Besides the mean values of the 10 min minima and maxima, 3 h maximum forces were calculated. Rather than taking the overall maximum line force from the simulations, a statistical 10 min maximum line force per 3 h has been determined and included in the figures. This statistical value has been calculated using a derived Gumbel distribution function of the 10 min maxima. In this way the most probable maximum mooring line force is obtained.

Of all the results obtained (van der Molen 2001), those of two typical simulation runs are presented in Figs. 4 and 5 and compared with the measured data. The most important loads were swell waves, with a significant wave height of about 0.30. m.

Discussion

The first impression from the presented figures (and all other simulation runs) is that the general resemblance between measurements and calculations is relatively good.

Observing Fig. 4 in more detail, it is noticed that (in this particular situation) the simulated line forces in the breast lines (see also Fig. 2) are on average 21% lower than the measured forces, with a maximum of 33% difference in line 13. For a partly loaded ship (Fig. 5) the difference between the measured and simulated line forces in breast lines reduces, but the simulated forces are still on average 12% lower than the measured forces, with a maximum of 23% differences in line 13.

Although these differences are not negligible, they are within the range of the expected accuracy of the simulations, taking into account the uncertainties of the prototype values for the loading condition and mooring line characteristics and uncertainties of the actual wave height and wave direction near the moored ship.

Analysis of Vessel Motions

A second part of the study was aimed at developing simplified expressions to calculate vessel motions. Previous research was focused on the relation between surge amplitude and long period wave height, schematizing the stiffness of the mooring line configuration into one value in the *x*-direction (Mol et al. 1986). This study tried to expand this work to other modes.

Vessel motions were not included in the prototype measurements. However, the output of the TERMSIM simulations includes detailed data of the motions of the moored ship. In case of a good resemblance between the measured and simulated line force data, the calculated motion data are assumed to reliably represent the prototype motions of the moored ship. However, this assumption can only be applied with any degree of confi-

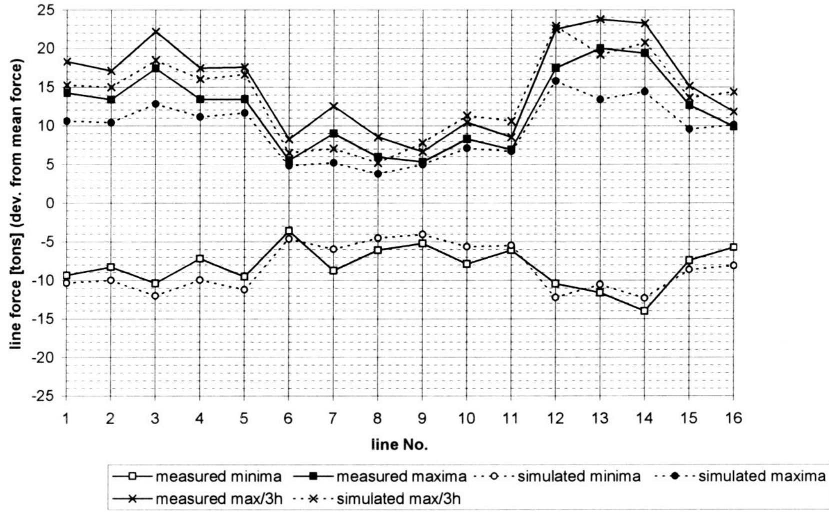

Date	Vessel	Environmental conditions		
		wind	tide	waves
19 July 1996	Standard loaded 125,000 m^3 LNG carrier 16 m water depth, T = 11.3 m	v = 4 m/s $\theta_v = 80°$	level = -0.5 m AHD u = 0.4 m/s $\theta_u = 120°$	$H_s = 0.27$ m $T_m = 14$ s $\theta_w = 198°$

Fig. 5. Comparison of line forces, loading condition 80%

dence to the dominant vessel motions, which are directly linked to the maximum line forces. From the analysis of measured and simulated line forces it was concluded that loads in breast lines are dominant over loads in spring lines, despite the wave direction, which was nearly head on. Hence vessel motions perpendicular to the berthing line are dominant over the surge motion.

The forces in breast lines and the vessel motion perpendicular to the berthing line were further analyzed. From Figs. 6 and 7 it follows that the yaw motion is almost entirely responsible for the forces in breast lines because the shape of the yaw spectrum is almost equal to the shape of the line-force spectra. The input wave spectrum was a JONSWAP spectrum, peak frequency 0.375 rad/s ($T_p = 16.8$ s). The spectra of other vessel motions show a much poorer resemblance to the spectrum of breast line forces and were concluded to be of less importance.

Hence it was decided to search for a relationship for the yaw motion of the moored ship. The most important parameters that influence the yaw motion are

1. Ship size: mass, displacement, and length;
2. Stiffness of fenders and mooring lines;

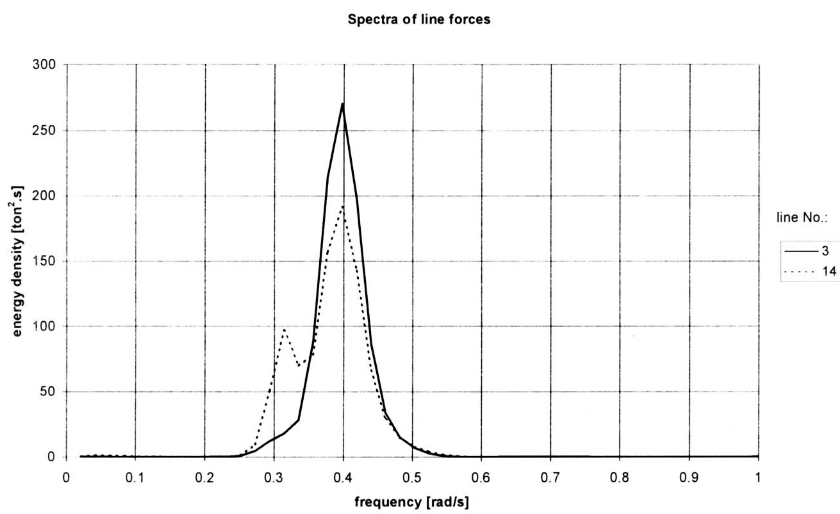

Date	*Vessel*	*Environmental conditions*		
		wind	*tide*	*waves*
2 August 1996	*Standard loaded 125,000 m^3 LNG carrier 20 m water depth, T = 11.3 m*	*v = 7.4 m/s* $\theta_v = 80°$	*level = 1.8 m AHD u = 0.2 m/s* $\theta_u = 120°$	*Hs = 0.28 m* $T_m = 14$ *s* $\theta w = 198°$

Fig. 6. Spectra of breast line force

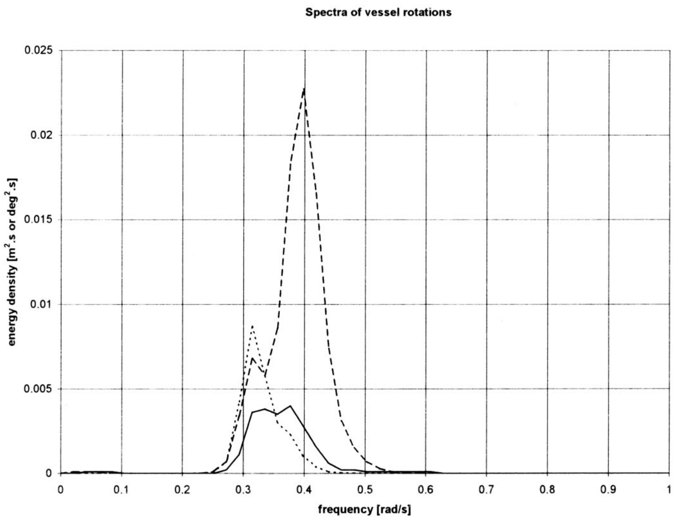

Fig. 7. Motion spectra

3. Wave height;
4. Wave period;
5. Wave direction; and
6. Water depth.

A large number of simulations were carried out to determine the relations between the yaw motion of the moored ship and the parameters mentioned above. Fig. 8 illustrates the yaw motion ($X_{6,s}$) of the moored ship depends on the rotational stiffness of the mooring system and on the frequency of the wave loads. The situation with stiffness $k_{66} = 100$ GNm/rad and $\omega_p = 0.40$ rad/s is approximately equal to the analyzed situation in Withnell Bay. Hence a formula to calculate the yaw motions based on the situation in Withnell Bay would lead to an upper-limit approach if the stiffness of the mooring system is not taken into account.

The relation between yaw amplitude and the wave height is linear in theory because the measured yaw motions are due to first-order wave forces, and according to Eq. (2), the first-order wave force is proportional to wave height.

The yaw motion is dependent not only on the wave period but also on the water depth. A relationship between yaw and wave length, which depends on both wave period and water depth, appeared to be more appropriate.

Yaw motions are negligible for long-crested waves head on. The relationship with wave direction is almost linear up to quartering waves. Maximum yaw occurs at a wave direction 60° from the bow, then decreases again for beam waves.

Based on the simulations to verify the yaw motions of a 125,000 m^3 LNG carrier, the following relationship has been derived:

$$X_{6,s} = C_{yaw} \cdot |\theta - 180°| \cdot L_p (L_p - C_L) \cdot H_s \tag{4}$$

where $X_{6,s}$=significant yaw motion (°); C_{yaw}, C_L=empirical coefficients (m^{-3}, m); θ=wave direction (°); L_p=peak wavelength of JONSWAP swell spectrum (s); and H_s=significant wave height of JONSWAP swell spectrum (m). The calculated motions are considered to be upper limit values because the effect of the stiffness of the mooring system on yaw is taken into account in a conservative way.

In order to make the expression valid for a wider range of vessel sizes, the wave length and wave height are made dimensionless by dividing with the ship length and the draft of the vessel, respectively. Furthermore, the wave length is written in terms of wave period and water depth with the assumption of shallow water, which is fairly reasonable for long swell waves in harbor basins. These assumptions lead to the following relation comprising dimensionless terms:

$$X_{6,s} = \tilde{C}_{yaw} \cdot |\theta - 180°| \cdot \frac{T_p \sqrt{gd}}{L_{PP}} \cdot \left(\frac{T_p \sqrt{gd}}{L_{PP}} - 0.4 \right) \cdot \frac{H_s}{T} \tag{5}$$

where $\tilde{C}_{yaw}$=dimensionless yaw coefficient (−); T_p=peak period of JONSWAP swell spectrum (s); g=acceleration of gravity (m/s^2); d=water depth (m); L_{PP}=length between perpendiculars (m); and T=draft of ship (m).

Notes:

- The unit of the calculated significant yaw motion is degrees, if $|\theta - 180°|$ is expressed in degrees.
- The dimensionless yaw coefficient, $\tilde{C}_{yaw}$, is 0.6 on average and varies from 0.4 to 0.7, based on both simulations and operation of the available measured data.

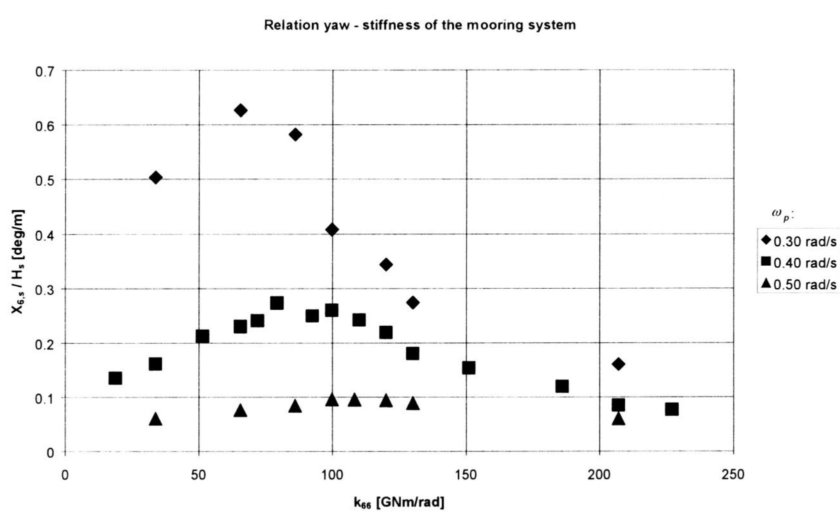

Fig. 8. Relation between yaw and stiffness in 6th mode

- The expression is an upper-limit approach with respect to the stiffness of the mooring system.
- The equation is valid for LNG carriers ranging in size from 70,000 to 170,000 m^3.
- The range of validity for wave direction is $135° < \theta < 170°$ and $190° < \theta < 225°$. For values of wave direction almost head on, Eq. (4) would give too low results because of the influence of directional spreading of the incident waves.
- The range of validity for peak periods is $12 \text{ s} < T_p < 22$ s.
- The range of validity for water depth is $1.25 \cdot T(\approx 14 \text{ m}) < d < 2 \cdot T(\approx 22 \text{ m})$.
- Incident waves from aft would lead to about 10 to 20% larger yaw motions.

With this expression a first-order estimate can be made of the expected yaw amplitude of a moored ship, on the basis of the wave conditions at the terminal location and the ship dimensions. Taking into account the stiffness of the mooring lines, in addition to a relatively simple expression for the significant line forces in the breast lines can be obtained:

$$F_{i,s} = F_{\text{pretension},i} + k_i \cdot X_{6,s} \cdot |x_i| \tag{6}$$

where $F_{i,s}$ = significant force in (breast) line i (N); $F_{\text{pretension},i}$ = pretension in line i (N); k_i = stiffness of line i in y-direction (N/m); $X_{6,s}$ = significant yaw amplitude (rad); and x_i = x-position of fairlead (m).

In this equation it is assumed that breast lines run perpendicular to the ship centerline.

It should be stressed that Eq. (4) has been derived from one set of prototype measurements only and that verification with other prototype or model data is needed. Until this has been done Eqs. (5) and (6) should be used cautiously.

Conclusions

The verification study of the simulation program TERMSIM has led to acceptable results concerning a loaded LNG ship moored to a jetty exposed to swell waves.

Based on the results of this study, an expression for yaw motions of a LNG carrier is made. The expression for the yaw motion mentioned in this paper [Eq. (5)] is part of the set of equations that can be used during preliminary terminal design studies.

Acknowledgment

The writers wish to thank Shell Global Solutions International BV for making available the prototype measurements used in this research project.

References

Ligteringen, H., and Moes, J. (2001). "Motions of moored ships in long waves." *Int. Conf. on Port and Maritime R&D and Technology*, Singapore.

Pinkster, J. A. (1980). "Low frequency second order wave exciting forces on floating structures." PhD thesis, Delft Univ. of Technology, Delft, The Netherlands.

Molen, W. (2001). "Computer simulation of the behavior of an LNG carrier moored to an open jetty." MSc thesis, Delft Univ. of Technology, Delft, The Netherlands.

van der, Mol, A., Ligteringen, H., and Waanders, A. J. (1986). "Motions of moored vessels, a statistical approach." *1st Australasian Port, Harbour and Offshore Engineering Conf.*, 141–145.

van Oortmerssen, G. (1976). "The motions of a moored ship in waves." PhD thesis, Delft Univ. of Technology, Delft, The Netherlands.

van Oortmerssen, G., Pinkster, J. A., and van den Boom, H. J. J., (1986). "Computer simulation of moored ship behavior." *J. Waterw., Port, Coastal, Ocean Eng.* 112(2), 296–308.